LA-UR- 00-5277

Title: High Temperature Stress Assessment in SCS-6/Ti-6A1-4V Composite Using Neutron Diffraction and Finite Element Modeling

Author(s): Partha Rangaswamy, MST-8

Submitted to: THERMEC 2000 International Conference
December 4-8, 2000
Las Vegas, Nevada

Los Alamos
NATIONAL LABORATORY

DISCLAIMER

DISCLAIMER

Portions of this document may be illegible in electronic image products. Images are produced from the best available original document.

High Temperature Stress Assessment in SCS-6/Ti-6Al-4V Composite using Neutron Diffraction and Finite Element Modeling

Partha Rangaswamy[1], Hahn Choo[1], Michael B. Prime[1], Mark A. M. Bourke[1], James M. Larsen[2]

[1] *Los Alamos National Laboratory, Los Alamos, NM 87545, U.S.A.*

[2] *Air Force Research Laboratory, Wright Patterson Airforce Base, Dayton, Ohio 45433, U.S.A*

Abstract

Thermal Residual stresses (TRS) in a continuous silicon carbide fiber reinforced (35 vol. %) titanium matrix composite were measured using neutron diffraction (ND). The TRS were determined in the matrix and fibers during heating from room temperature to 1170K. An elasto-viscoplastic finite element analysis was used to predict TRS by allowing matrix creep matrix and the thermal history followed during the course of ND measurements. The comparison of TRS between FEM predictions and ND measurements showed good agreement across the temperature region. At room temperature, axial and transverse stresses (parallel and perpendicular to the fibers) were in the ratio of ~3:1, both in the matrix and fiber phases, respectively. With increase in temperature the residual stresses relaxed linearly to ~ 900K, beyond which the stresses remained close to zero to 1170 K.

1.   Introduction

Continuous silicon carbide fiber (SCS-6) reinforced titanium alloy (Ti-6Al-4V) matrix composites (TMCs) are consolidated using a hot-isostatic-process (HIP) at a processing temperature (T_P) of 1115 K. Due to the larger than two-fold mismatch in the coefficients of thermal expansion (CTE) between the SiC (3.2×10^{-6}/ K at room temperature) and the titanium (8.78×10^{-6}/K at room temperature) residual stresses develop on cooling to room temperature (T_R) from the processing temperature. Despite extensive room temperature characterization (T_R) [1-8], only a few experimental studies have addressed the stress evolution as a function of temperature (e.g SCS-6/Ti-14Al-21Nb [9], SCS-6/Ti-6Al-4V [10]). Where high temperature measurements have been made, neutron diffraction (ND) is commonly used because stresses in both the matrix and the fiber reinforcement are obtained simultaneously. However, because of the speed of cooling from fabrication temperatures, the general practice has been to determine stresses during a slow reheat towards the processing temperature (T_P). Particularly at higher temperatures in the regime of (800 – 1170K [10]) this means that the real-time inelastic relaxation (creep) that occurs during the measurement must be addressed [10, 11]. In this paper we used stresses measured in SCS-6/Ti-6Al-4V TMC [10] as a function of temperature to validate a finite element model (FEM) which includes time dependent (elasto-viscoplastic) response. Although numerous FEM analyses have predicted residual stresses at elevated temperatures, few address the time-and path-dependency of the residual stress [1,11-13]. Direct considerations of real-time affects should clearly be important in high temperature creep or thermal fatigue environments.

2.   Material

The continuous SiC fiber-reinforced Ti-6Al-4V matrix composite, under study, consisted of eight plies of unidirectionally aligned SCS-6 fibers (140μm in diameter, 35 vol.%). Panels of the composite and of monolithic Ti-6Al-4V (approximately 100mm long, 15mm wide and 2mm thick) were fabricated by the foil-fiber-foil process at Textron Specialty Materials [14]. The individual panels were subsequently consolidated by hot isostatic pressing in a vacuum sealed stainless steel can at 1115K, 100MPa for 2 hours followed by a slow furnace cool.

3.   Neutron Diffraction

Strain evolution during heating was characterized *in situ* using the Neutron Powder Diffractometer at the Manuel Lujan Jr. Neutron Scattering Center in Los Alamos National Laboratory. Neutron diffraction provides bulk average measurements due to the typically large depth of penetration into most engineering materials (e.g. ~1cm for titanium with $\lambda = 1.4$ Å). Therefore, it is an effective, non-destructive technique for measuring 'bulk' internal

strains in metal matrix composites [15, 16]. Furthermore, by using the spallation neutron source, all possible lattice planes are recorded in each measurement [16].

Details of the experimental analysis including the measurement procedure, acquisition and analysis of diffraction data are well documented [10, 15-19]. However, the following comparison of measurements with the model merits a brief description of how strain and stress are determined from the diffraction data.

Diffraction patterns were acquired from standards of the monolithic Ti-6-4 and SiC fibers as well as from the composite from room temperature to 1170K at intervals of about 100K in an argon atmosphere. Heating between temperatures took about 5 minutes. Prior to collecting data, samples were held for 15 minutes at each new temperature to ensure thermal equilibrium. Diffraction patterns were collected for 105 minutes for both the Ti-6-4 monolithic and the composite following an identical time-temperature profile. Matching the time-temperature profile ensures a fair comparison between samples in which time-dependent relaxation and phase transformations are expected. Since the SiC behavior is assumed to be time-independent (i.e. neither creep relaxation nor phase transformation are expected within the fiber), measurements for fibers were performed at the same temperatures but only for 60 minutes at each temperature.

From the diffraction patterns lattice parameters for the α-Ti (hcp) and SiC (fcc) were obtained by Rietveld analysis [20]. For the cubic SiC, the bulk-average elastic strains were determined using, $\varepsilon_{bulk-avg} = (a-a_0)/a_0$, where a and a_0 are the *temperature-specific* lattice parameters of the SiC in the composite or standard, respectively. For the hexagonal α-Ti phase, the a- and c-axes strains were combined to give a bulk average strain $\varepsilon_{bulk-avg} = (2\varepsilon_a + \varepsilon_c)/3$, where ε_a and ε_c are the bulk-average strains along a- and c-axes, respectively. Although empirical this approach has previously shown to be justifiable [17,18,21].

The measured bulk-average elastic phase strains were converted to stress. Using Hooke's law (subject to the assumption of transverse isotropy), where the axial (σ_A) and transverse (σ_T) stresses are calculated using,

$$\sigma_A = \frac{E}{(1+v)(1-2v)}((1-v)\varepsilon_A + 2v\varepsilon_T) \qquad (1)$$

$$\sigma_T = \frac{E}{(1+v)(1-2v)}(v\varepsilon_A + \varepsilon_T) \qquad (2)$$

where E is temperature dependent Young's modulus (Table 1) and v is Poisson's ratio both of which are assumed isotropic. v was assumed temperature independent having a value of 0.31 for Ti-6Al-4V and 0.25 for SiC, respectively [19]. ε_A and ε_T are the measured axial and transverse strains, respectively.

4.   Finite Element Modeling

The unit cell Finite element model (FEM) used a generalized plane strain approach assuming a rectangular fiber array implemented using the commercial finite-element code ABAQUS [22]. The unit cell comprised quarter symmetry and used 20-node bi-quadratic 3-D solid elements (C3D20R), which represents a transverse cross-section through a continuous, infinitely long composite, **Fig. 1**. The left and bottom edges were constrained from moving in the horizontal and vertical directions, respectively, to enforce symmetry. The top and right edges were constrained using multi-point constraints to remain horizontal and vertical, respectively, but were permitted translation normal to the edge. The fiber/matrix interface was modeled as a perfectly bonded composite [1,13].

Measured plasticity values were used for the Ti-6Al-4V matrix (Table 1) where σ_y is 0.2% compressive yield stress, E is the Young's modulus and E_f is the flow modulus describing the strain hardening [19]. Plasticity within ABAQUS was described using incremental plasticity, Von Mises yield surface and the associated flow rule. The matrix steady
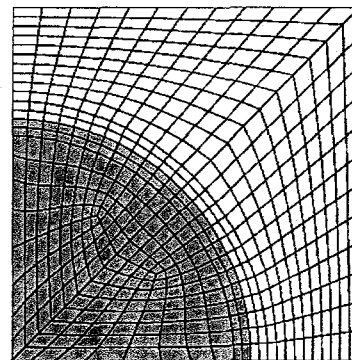

Fig. 1: Schematic of unit cell 3-D FEM model.

state creep rate (sec^{-1}), $\dot{\varepsilon}^{cr}$, was defined by

$$\dot{\varepsilon}^{cr} = B\sigma^n \exp\left(\frac{-Q}{RT}\right)$$

(3)

where, B is a constant (=1x10^{-6}), σ is the applied stress (MPa), n is the stress exponent (=3.4), Q is apparent creep activation energy (=301KJ/mol), R is the gas constant (= 8.314J/degree·mol) and T is the absolute temperature [1]. The SiC fiber was treated as purely elastic, **Table 1**.

The thermal loading cycles imposed in the FEM model during cooling and heating were matched to the thermal history during fabrication and during the subsequent ND measurements. In addition, we assumed uniform temperature changes throughout the unit cell thereby ignoring non-uniform cooling effects.

The FE results, which are spatially resolved within the model, were volume averaged over the entire phase specific cross-section of the unit cell to provide a comparison to the ND results. The volume averaged stress along a chosen direction, $\overline{\sigma}$, was calculated using a previously reported scheme [17];

$$\overline{\sigma} = \frac{1}{V}\int_V \sigma dV$$

(4)

where, σ is a stress component in the *axial or transverse* direction and V is a volume of a phase.

Silicon Carbide (SCS-6)			Ti-6Al-4V				
Temp. K	Young's Modulus (GPa)	CTE (10^{-6}/K)	Temp. K	Young's Modulus (GPa)	σ_y, Yield stress (MPa)	E$_f$, Flow Modulus (GPa)	CTE (10^{-6}/K)
294	393	3.20	296	125	1000	0.7	8.78
366	390	3.34	533	110	630	2.2	9.83
477	386	3.54	589	100	630	2.2	10.01
589	382	3.74	700	100	525	2.2	10.71
700	378	3.92	755	80	500	1.9	11.10
811	374	4.09	811	74	446	1.9	11.22
922	370	4.25	923	55	300	1.9	11.68
1033	365	4.41	1073	27	45	2	12.21
1144	361	4.55	1098	20	25	2	12.29
1366	354	4.78	1123	5	5	2	12.37

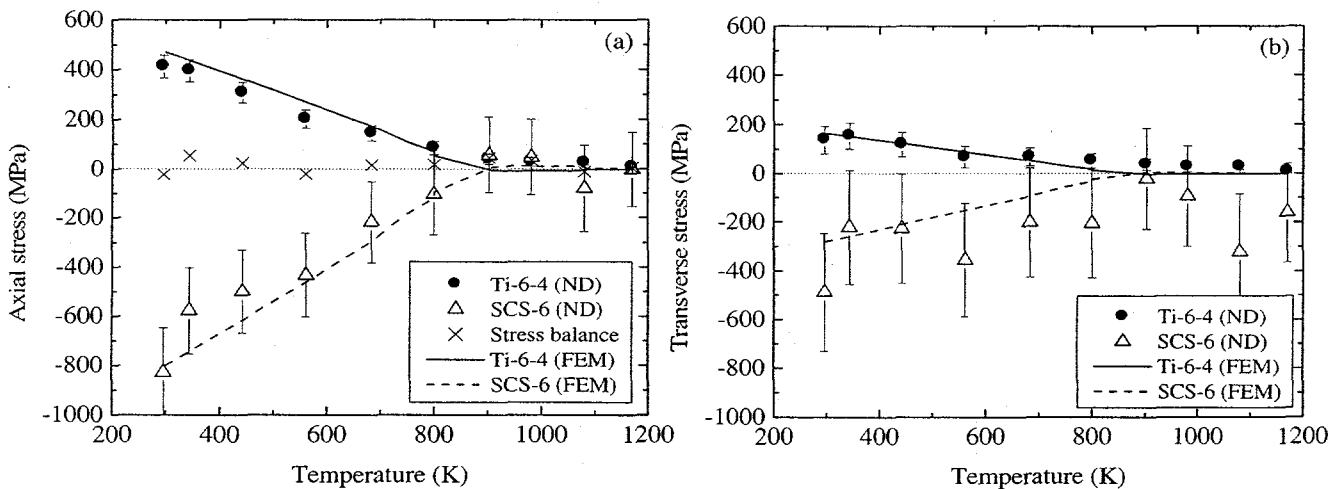Table 1: Material properties used in the FEM model.

Fig. 2: FEM and ND stresses in the Ti-6Al-4V matrix and SCS-6 fibers: (a) axial (b) and transverse. The stress balance (x) is illustrated in 2a for the ND axial stresses.

5. Results and Discussion

5.1 Neutron Diffraction and Elastic-Viscoplastic FEM

In **Fig. 2(a,b)**, ND measured and FEM predicted stresses are shown for the 'axial' and 'transverse' stresses in the composite matrix (α-Ti) and fibers (SiC) as a function of temperature. The symbols represent the measurement values and the lines are fits to the FEM predicted values. It is observed that the FE predictions show remarkably good agreement with the experimental data across the temperature region. The stress-balance (x), commonly used as a check on the accuracy of the measurements, shows that the mean phase axial stresses for the two phases are as expected in equilibrium (**Fig. 2a**) [21].

At room temperature: The axial stress as determined by ND in the matrix is tensile (410±45 MPa) while the fibers are in compression (-830±180 MPa). Similarly, the transverse stress in the matrix is tensile (140±55 MPa) and compressive in the fibers (–490±240 MPa). The axial residual stresses are three times the transverse stresses in both the phases at room temperature (Note that the transverse stresses are an average of radial and hoop stress components along the transverse direction).

RT<T≤900K: In the axial direction (**Fig. 2a**) as the temperature was increased, the ND measured stresses in both phases relax in direct proportion to the change in temperature reaching zero stress (T_s–stress relaxation temperature) between 800-900K. In the transverse direction (**Fig. 2b**), the trend is similar. Note, the fiber stresses show scatter with a large uncertainty ($\approx$ ±200 MPa). The ND measurements are tracked closely supported by the FEM linear relaxation of axial and transverse stresses with increasing temperature. Note, the FEM predicted relaxation temperature (T_s) is ~ 900K in both axial and transverse directions.

800<T≤1170K: Beyond the apparent relaxation temperature it appears from the ND that the axial stresses are completely relaxed and remain constant. The same appears to be true for the transverse stresses in the matrix, but the values for the fiber show large error bars. The ND measurements agree with the FEM predictions, which show no further stress changes to 1170K. One may reasonably conclude that beyond 900K creep relaxes the geometric incompatibility caused by differing coefficient of thermal expansion. In addition, at these temperatures (~900 – 1170K) the elastic modulus, yield stress and work hardening are small (compared to RT) and therefore any stress accumulation in the TMC at these temperatures are also small.

It should be noted that even though neutron diffraction strains were measured in both α and β phases of Ti-6Al-4V [10] only stresses determined for the α phase are reported here. Lack of space precludes a detailed explanation but we note up to the phase transformation temperature (~ 800K) the α phase is the major constituent phase (90 % V_f) exhibiting significantly higher stress than the β phase. The application of rule of mixture in determining the total stress in the titanium showed that the contribution of β stress was small.

5.2 Elastic-Viscoplastic vs. Elastic-Plastic FEM modeling

We have shown the application of ND measurements to validate an elasto-viscoplastic FEM. However, this assessment would not be complete without contrasting its merits with an elasto-plastic analysis. Traditionally, ND measurements have been used to validate FEM models using an elasto-plastic analysis. The rationale is that it is simpler analysis in the absence of creep property data. In an elasto-plastic analysis the inelastic deformation is solely due to plasticity, which develops in a time independent fashion. Typically the residual stresses at room temperature are matched by choosing a stress free temperature (T_S) that is significantly less than the fabrication temperature. This reduces the ΔT (difference in temperature) imposed during cooling so that the model does not overestimate the room temperature residual stress because creep is not considered in the model. This approach was applied to SCS-6/Ti-24Al-21Nb [9] TMC where reasonable agreement between an elasto-plastic and neutron diffraction data was achieved.

In **Fig. 3** we compare elasto-viscoplastic matrix predicted axial stress evolution with two elasto-plastic calculations using T_s of 1115K (i.e. HIPing temperature) and 836K ($0.75T_P$). The choice of 836K was dictated by previous research [23], which suggested that by using ~0.7-0.8 times the absolute processing temperature an elasto-plastic analysis could mimic elasto-viscoplastic analysis. The room temperature axial residual stresses as measured by ND are compared to 640 MPa for $T_s = 1115$K and 400 MPa for Ts = 836 K respectively. In our case, the elasto-viscoplastic analysis has been validated by ND. Thus, it is apparent that 0.75 T_P underestimates the room temperature stresses.

From **Fig. 3** it can be seen that an appropriate choice of T_s between 0.75 T_P and T_P, would be to provide similar results as the elasto-viscoplastic analysis. The close match of a stress value at room temperature and during the heat up cycle between elasto-plastic model and experiment data does not necessarily validate a model, because, in many cases T_S may be function of the materials properties (e.g. yield and creep strength of the matrix), fiber volume fraction and cooling rate. Therefore, for further application of elasto-plastic models to the study of high temperature behavior, it is important that the model be checked using re-heat data with which the temperature-, time- and path-dependent behavior can be validated (Although axial stresses are shown for the FEM predictions, the transverse stresses showed identical trends).

Fig. 3: FEM predicted axial stresses for elastic-plastic and elasto-viscoplastic matrices.

Necessarily elasto-plastic predictions of stress relaxation as a function of temperature introduce assumptions concerning T_S. However, assuming that material properties are available – creep calculations are quite feasible and can accurately predict stress response without any inherent assumptions.
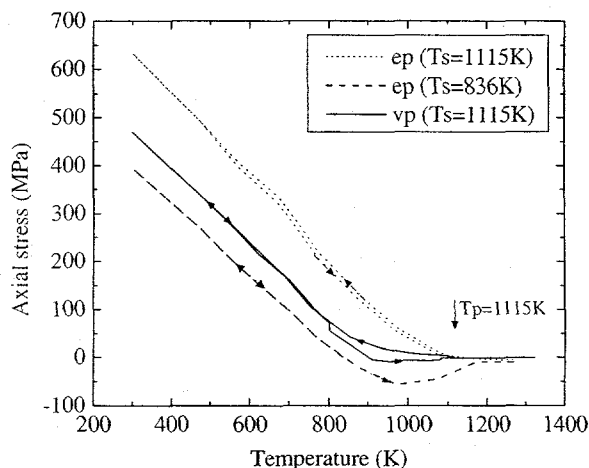
6. Summary and Conclusions

The thermal residual stress evolution during heating of a SCS-6/Ti-6Al-4V TMC was characterized using *in situ* high temperature neutron diffraction. The experimental results were used to validate FEM model based on elasto-viscoplastic (which used both time and path dependency consideration within the model). There was good agreement between the ND measurements and the FEM predictions between room temperature and 1170K. At room temperature, the axial and transverse residual stresses were in the ratio of ~3:1, between the matrix and fiber phases, respectively. With increase in temperature the residual stresses relaxed linearly up to ~ 900K. Beyond this temperature the stresses remained closed to zero up to 1170 K.

7. Acknowledgements

8. References

1. R.P. Nimmer, R.J. Bnakert, E.S. Russel, G.A. Smith and P.K. Wright, J. Comp. Tech. Res. 13, 3 (1991).
2. J.F. Durodola and B. Derby, Acta Metall. Mater. 42, 1525 (1994).
3. S.M. Pickard and D.B. Miracle, Mater. Sci. Eng. A203, 59 (1995).

4. P. Rangaswamy, M.B. Prime, M. Daymond, M.A.M. Bourke, B. Clausen, H. Choo and N. Jayaraman, Mater. Sci. Eng. A259, 209 (1999).
5. S.H. Thomin, P.A. Noel and D.C. Dunand, Metall. Mater. Trans. 26A, 883 (1995).
6. P. Rangaswamy, M.A.M. Bourke, P.K. Wright, N. Jayaraman, E. Kartzmark and J.A. Roberts, Mater. Sci. Eng. A224, 200 (1997).
7. P.J. Withers and A.P. Clarke, Acta Mater. 46, 6585 (1998).
8. D.B. Miracle and B.S. Majumdar, Metall. Mater. Trans. A30, 301 (1999).
9. Saigal, D.S. Kupperman and S. Majumdar, Mater. Sci. Eng. A150, 59 (1992).
10. H. Choo, P. Rangaswamy, Mark A. M. Bourke, Scripta Materialia , v. 42(#2) pp. 175-181, Dec 31, (1999).
11. H. Choo, M. A. M. Bourke, P. G. Nash and M. R. Daymond, in Ceramic Engineering & Science Proc., 24th Annual Conference on Composites, Advanced Ceramics, Materials and Structures: A, Edited by T. Jessen and E. Ustundag, Cocoa Beach, Florida, vol. 21 (3), pp. 627-634, (2000).
12. M.N. Tamin, D. Zheng and H. Chonem, J. Comp. Tech. Res. 16, p314 (1994).
13. C.R. Ananth, S. Mukherjee and N. Chandra, J. Comp. Tech. Res. 19, p134 (1997).
14. Textron Specialty Materials, Lowell, MA, 01851, USA
15. H. Choo, M. Bourke, P. Nash, M. Daymond and N. Shi, Mater. Sci. Eng. A264, 108 (1999).
16. M.A.M. Bourke, J.A. Goldstone and T.M. Holden, Measurement of Residual and Applied Stress Using Neutron Diffraction, Kluwer Academic Publishers, Netherlands, 369 (1992).
17. A.D. Krawitz, R.A. Winholtz and C.M. Weisbrook, Mater. Sci. Eng. A206, 176 (1996).
18. M.R. Daymond, M.A.M. Bourke and R.B. Von Dreele, J. Appl. Phys. 85, 739 (1999).
19. P. Rangaswamy, M.B. Prime, M. Daymond, M.A.M. Bourke, B. Clausen, H. Choo and N. Jayaraman, Mater. Sci. Eng. A259, 209 (1999).
20. A.C. Larson and R.B. Von Dreele, GSAS (LAUR 86-748), Los Alamos National Laboratory, Los Alamos, NM, (1986).
21. A.D. Krawitz, Measurement of Residual and Applied Stress Using Neutron Diffraction, Kluwer Academic Publishers, London, 405 (1992).
22. ABAQUS User's Manual (Hibbitt, Karlsson & Sorensen, Pawtucket, RI, (1996).
23. J.L. Kroupa and R.W. Neu, "The nonisothermal viscoplastic behavior of a titanium-matrix composite", Composite Engineering, vol. 4, pp. 965-977, (1994).